Multiphoton antiresonance in large-spin systems

C. Hicke and M. I. Dykman

Department of Physics and Astronomy, Michigan State University, East Lansing, Michigan 48824, USA
(Received 24 April 2007; published 21 August 2007)

We study nonlinear response of a spin $S > 1/2$ with easy-axis anisotropy. The response displays sharp dips or peaks when the modulation frequency is adiabatically swept through multiphoton resonance. The effect is a consequence of a special symmetry of the spin dynamics in a magnetic field for the anisotropy energy $\propto S_z^2$. The occurrence of the dips or peaks is determined by the spin state. Their shape strongly depends on the modulation amplitude. Higher-order anisotropy breaks the symmetry, leading to sharp steps in the response as function of frequency. The results bear on the dynamics of molecular magnets in a static magnetic field.

I. INTRODUCTION

Large-spin systems have been attracting much attention recently. Examples are $S=3/2$ and $S=5/2$ Mn impurities in semiconductors and Mn- and Fe-based molecular magnets with electron spin $S=10$ and higher. Nuclear spins $I=3/2$ have also been studied, and radiation-induced quantum coherence between the spin levels was observed.[1] An important feature of large-spin systems is that their energy levels may be almost equidistant. A familiar example are spins in a strong magnetic field in the case of a relatively small magnetic anisotropy, where the interlevel distance is determined primarily by the Larmor frequency. Another example are low-lying levels of large-S molecular magnets for small tunneling. As a consequence of the structure of the energy spectrum, external modulation can be close to resonance with many transitions at a time. This should lead to coherent nonlinear resonant effects that have no analog in two-level systems.

The effects of a strong resonant field on systems with nearly equidistant energy levels have been studied for weakly nonlinear oscillators. These studies concern both coherent effects, which occur without dissipation,[2–4] and incoherent effects, in particular, those related to the oscillator bistability and transitions between coexisting stable states of forced vibrations. In the absence of dissipation, a nonlinear oscillator may display multiphoton antiresonance in which the susceptibility shows a dip or a peak as a function of modulation frequency.[5]

In the present paper, we study resonantly modulated spin systems with $S > 1/2$. Of primary interest are systems with uniaxial magnetic anisotropy, with the leading term in the anisotropy energy of the form of $-DS_z^2/2$. We show that the coherent response of such spin systems displays peaks or dips when the modulation frequency adiabatically passes through multiphoton resonances. The effect is nonperturbative in the field amplitude. It is related to the special conformal property of the spin dynamics in the semiclassical limit. It should be noted that the occurrence of antiresonance for a spin does not follow from the results for the oscillator. A spin can be mapped onto a system of two oscillators rather than one; the transition matrix elements for a spin and an oscillator are different as are the energy spectra.

We show that the coherent response of a spin is sensitive to terms of higher order in S_z in the anisotropy energy. In addition, there is a close relation between the problem of resonant high-frequency response of a spin and the problem of static spin polarization transverse to the easy axis. Spin dynamics in a static magnetic field has been extensively studied both theoretically and experimentally.[6–15] One of the puzzling observations on magnetization switching in molecular magnets, which remained unexplained except for the low-order perturbation theory, is that the longitudinal magnetic field at which the switching occurs is independent of the transverse magnetic field.[10] The analysis presented below provides an explanation which is nonperturbative in the transverse field and also predicts the occurrence of peaks or dips in the static polarization transverse to the easy axis as the longitudinal magnetic field is swept through resonance.

The onset of strong nonlinearity of the response due to near equidistance of the energy levels can be inferred from Fig. 1(a). It presents a sketch of the Zeeman levels of a spin E_m ($-S \leq m \leq S$) in a strong magnetic field along the easy magnetization axis $\hat{z}$. The spin Hamiltonian is

$$H_0 = \omega_0 S_z - \tfrac{1}{2}DS_z^2 \quad (\hbar = 1), \qquad (1)$$

where ω_0 is the Larmor frequency. For comparatively weak anisotropy, $DS \ll \omega_0$, the interlevel distances $E_{m+1} - E_m$ are close to each other and change linearly with m.
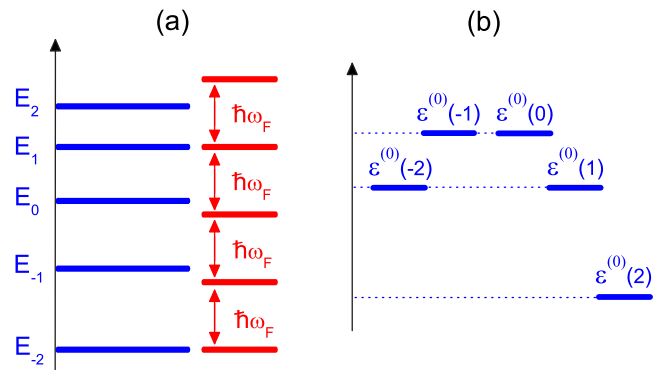

FIG. 1. (Color online) Three-photon resonance in an $S=2$ system in the limit of a weak ac field. (a) Spin energy levels E_m and N-photon energies $n\hbar\omega_F$. (b) Quasienergies in the limit of zero modulation amplitude, $\varepsilon^{(0)}(m) = E_m - m\hbar\omega_F$; the pairwise degenerate levels correspond to one- and three-photon resonance, respectively.

A transverse periodic field leads to transitions between neighboring levels. An interesting situation occurs if the field frequency ω_F is close to ω_0 and there is multiphoton resonance in the mth state: $N\omega_F$ coincides with the energy difference $E_{m+N} - E_m$, $N > 1$. The amplitude of the resonant N-photon transition in this case is comparatively large, because the transition goes via N sequential one-photon virtual transitions which are all almost resonant. Therefore, one should expect a comparatively strong multiphoton Rabi splitting already for a moderately strong field.

A far less obvious effect occurs in the coherent response of the system, that is, in the magnetization at the modulation frequency or, equivalently, the susceptibility. As we show, the expectation value of the susceptibility displays sharp spikes at multiphoton resonance. The shape of the spikes very strongly depends on the field amplitude.

The paper is organized as follows. In Sec. II, we study the quasienergy spectrum and the response of a spin with quadratic in S_z anisotropy energy. We show that at multiphoton resonance, not only multiple quasienergy levels are crossing pairwise, but the susceptibilities in the resonating states are also crossing. In Sec. III, we show that multiphoton transitions, along with level repulsion, lead to the onset of spikes in the susceptibility and find the shape and amplitude of the spikes as functions of frequency and amplitude of the resonant field. In Sec. IV, we present a WKB analysis of spin dynamics, which explains the simultaneous crossing of quasienergy levels and the susceptibilities beyond perturbation theory in the field amplitude. In Sec. V, the role of terms of higher order in S_z in the anisotropy energy is considered. Section VI contains concluding remarks.

II. LOW-FIELD SUSCEPTIBILITY CROSSING

A. Quasienergy spectrum

We first consider a spin with Hamiltonian H_0 [Eq. (1)], which is additionally modulated by an almost resonant ac field. The modulation can be described by adding to H_0 the term $-S_x A \cos \omega_F t$, where A characterizes the amplitude of the ac field. As mentioned above, we assume that the field frequency ω_F is close to ω_0 and that $\omega_F, \omega_0 \gg D, A, |\omega_F - \omega_0|$.

It is convenient to describe the modulated system in the quasienergy, or Floquet representation. The Floquet eigenstates $|\psi_\varepsilon(t)\rangle$ have the property $|\psi_\varepsilon(t+\tau_F)\rangle = \exp(-i\varepsilon\tau_F)|\psi_\varepsilon(t)\rangle$, where $\tau_F = 2\pi/\omega_F$ is the modulation period and ε is quasienergy. For resonant modulation, quasienergy states can be found by changing to the rotating frame using the canonical transformation $U(t) = \exp(-i\omega_F S_z t)$. In the rotating wave approximation, the transformed Hamiltonian is

$$H = -\delta\omega \, S_z - \frac{1}{2}DS_z^2 - \frac{1}{2}AS_x,$$

$$\delta\omega = \omega_F - \omega_0. \tag{2}$$

Here, we disregarded fast-oscillating terms $\propto A \exp(\pm 2i\omega_F t)$.

The Hamiltonian H has a familiar form of the Hamiltonian of a spin in a scaled static magnetic field with components $\delta\omega$ and $A/2$ along the $\hat{\mathbf{z}}$ and $\hat{\mathbf{x}}$ axes, respectively. Much theoretical work has been done on spin dynamics described by this Hamiltonian in the context of molecular magnets.

The eigenvalues of H give quasienergies of the modulated spin. In the weak modulating field limit, $A \to 0$, the quasienergies are shown in Fig. 1(b). In this limit, spin states are the Zeeman states, i.e., the eigenstates $|m\rangle^{(0)}$ of S_z, with $-S \leq m \leq S$. The interesting feature of the spectrum, which is characteristic of the magnetic anisotropy of the form DS_z^2, is that several states become simultaneously degenerate pairwise for $A = 0$.[10,11] From Eq. (2), the quasienergies $\varepsilon^{(0)}(m)$ and $\varepsilon^{(0)}(m+N)$ are degenerate if the modulation frequency is

$$\delta\omega = \delta\omega_{m;N}, \quad \delta\omega_{m;N} = -D\left(m + \frac{1}{2}N\right). \tag{3}$$

Condition (3) is simultaneously met for all pairs of states with given $2m+N$. It coincides with the condition of N-photon resonance $E_{m+N} - E_m = N\omega_F$. In what follows, N can be positive and negative. There are $4S-1$ frequency values that satisfy condition (3) for a given S.

The field $\propto A$ leads to transitions between the states $|m\rangle^{(0)}$ and to quasienergy splitting. The level splitting for the Hamiltonian (2) was calculated earlier.[11] For multiphoton resonance, it is equal to twice the multiphoton Rabi frequency $\Omega_R(m;N)$,

$$\Omega_R(m;N) = |A/2D|^{|N|} \, |D|$$
$$\times \left[\frac{(S+m+N)!(S-m)!}{(S+m)!(S-m-N)!}\right]^{(1/2)\text{sgn} \, N} \frac{1}{2(|N|-1)!^2}. \tag{4}$$

The N-photon Rabi frequency (4) is $\propto A^{|N|}$, as expected. We note that the amplitude A is scaled by the anisotropy parameter D, which characterizes the nonequidistance of the energy levels and is much smaller than the Larmor frequency. Therefore, Ω_R becomes comparatively large already for moderately weak fields $A \sim D$.

We denote the true quasienergy states as $|\nu\rangle$, with integer or half-integer ν such that $-S \leq \nu \leq S$. The quasienergies ε_ν do not cross. One can enumerate the states $|\nu\rangle$ by thinking of them as the adiabatic states for slowly increasing $\delta\omega$, starting from large negative $\delta\omega$. For $-\delta\omega/DS \gg 1, |A|/D$, the states $|\nu\rangle$ are very close to the Zeeman states $|\nu\rangle^{(0)}$, with ν being the eigenvalue of S_z. This then specifies the values of ν for all $\delta\omega$.

If the field is weak, the states $|\nu\rangle$ are close to the corresponding Zeeman states, $|\nu\rangle \approx |m\rangle^{(0)}$, for all $\delta\omega$ except for narrow vicinities of the resonant values $\delta\omega_{m;N}$ given by Eq. (3). The relation between the numbers ν and m for $|\nu\rangle \approx |m\rangle^{(0)}$ is

$$\nu = m + \sum_N{}' \theta(\delta\omega - \delta\omega_{m;N})\text{sgn} \, N, \tag{5}$$

where N runs from $-S-m$ to $S-m$; the term $N=0$ is eliminated, which is indicated by the prime over the sum; $\theta(x)$ is the step function. In obtaining Eq. (5), we took into account that, for weak fields, only neighboring quasienergy levels ε_ν
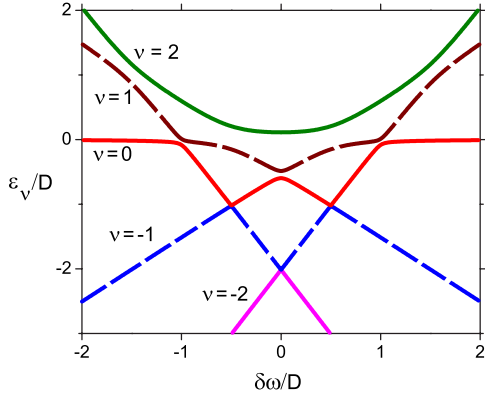
FIG. 2. (Color online) Quasienergy levels ε_ν for a spin-2 system as functions of detuning $\delta\omega/D$ for the scaled field amplitude A/D =0.3. The levels anticross pairwise at multiphoton resonances given by Eq. (3). The unperturbed quasienergies (the limit A=0) correspond to straight lines $\varepsilon^{(0)}(m) = -\delta\omega\,m - Dm^2/2$.

and $\varepsilon_{\nu\pm1}$ come close to each other. Equation (5) defines the state enumerating function $m(\nu)$.

The enumeration scheme and the avoided crossing of the quasienergy levels are illustrated in Fig. 2. For the chosen S=2, the anticrossing occurs for seven frequency values, as follows from Eq. (3). The magnitude of the splitting strongly depends on N: the largest splitting occurs for one-photon transitions. It is also obvious in Fig. 2 that several levels experience anticrossing for the same modulation frequency.

B. Susceptibility and quasienergy crossing

Of central interest to us is the nonlinear susceptibility of the spin. We define the dimensionless susceptibility χ_ν in the quasienergy state $|\nu\rangle$ as the ratio of the expectation value of the appropriately scaled magnetization at the modulation frequency to the modulation amplitude,

$$\chi_\nu(\omega_F) = \langle\nu|S_-|\nu\rangle/A. \tag{6}$$

In the weak-field limit, $A \to 0$,

$$\chi_\nu(\omega_F) = \frac{m(2\,\delta\omega + Dm) + DS(S+1)}{4(\delta\omega + Dm)^2 - D^2}, \tag{7}$$

where m and ν are related by Eq. (5); in fact, Eq. (7) gives the susceptibility in the perturbed to first order in A Zeeman state $|m\rangle^{(0)}$.

A remarkable feature of Eq. (7) is the susceptibility crossing at multiphoton resonance. The susceptibilities in Zeeman states $|m\rangle^{(0)}$ and $|m+N\rangle^{(0)}$ are equal where the unperturbed quasienergies of these states are equal, $\varepsilon^{(0)}(m)=\varepsilon^{(0)}(m+N)$, i.e., where the frequency detuning is $\delta\omega=\delta\omega_{m;N}$. In terms of the adiabatic states $|\nu\rangle$, for such $\delta\omega$ we have from Eqs. (5) and (7) $\chi_\nu(\omega_F)=\chi_{\nu'}(\omega_F)$ for $\nu'=\nu+\mathrm{sgn}\,N$.

A direct calculation shows that simultaneous crossing of the susceptibilities and quasienergies occurs also in the fourth order of the perturbation theory provided $N\geqslant3$. Numerical diagonalization of the Hamiltonian (2) indicates that it persists in higher orders, too, until level repulsion due to multiphoton Rabi oscillations comes into play.

The susceptibility χ_ν is immediately related to the field dependence of the quasienergy ε_ν. Since $\langle\nu|S_+|\nu\rangle=\langle\nu|S_-|\nu\rangle$, from the explicit form of the Hamiltonian (2) we have

$$\chi_\nu = -2A^{-1}\,\partial\varepsilon_\nu/\partial A. \tag{8}$$

Simultaneous crossing of the susceptibilities and quasienergies means that, for an N-photon resonance, the Stark shift of resonating states is the same up to order $N-1$ in A; only in the Nth order the levels ε_ν and $\varepsilon_{\nu+\mathrm{sgn}\,N}$ become split [by $2\Omega_R(m;N)$]. Respectively, the susceptibilities χ_ν and $\chi_{\nu+\mathrm{sgn}\,N}$ coincide up to terms $\propto A^{|N|-3}$. The physical mechanism of this special behavior is related to the conformal property of the spin dynamics, as explained in Sec. IV.

Equation (7) does not apply in the case of one-photon resonance, N=1: it gives $|\chi_\nu| \to \infty$ for $\delta\omega \to \delta\omega_{m;1}$. This is similar to the case of one-photon resonance in a two-level system, where the behavior of the susceptibility is well understood beyond perturbation theory. Interestingly, the lowest-order perturbation theory does not apply also at exact two-photon resonance, $\delta\omega=\delta\omega_{m;2}$, as discussed below, even though Eq. (7) does not diverge.

III. ANTIRESONANCE OF THE MULTIPHOTON RESPONSE

The field-induced anticrossing of quasienergy levels at multiphoton resonance is accompanied by lifting the degeneracy of the susceptibilities. It leads to the onset of a resonant peak and an antiresonant dip in the susceptibilities as functions of frequency $\delta\omega$. The behavior of the quasienergy levels and the susceptibilities is seen in Fig. 3. For small field amplitude A, the multiphoton Rabi frequency $\Omega_R \propto A^{|N|}$ is small, and the quasienergies of interest ε_ν and $\varepsilon_{\nu+1}$ [with $m(\nu+1)-m(\nu)=N$] come very close to each other at resonant $\delta\omega$, as do also the susceptibilities χ_ν and $\chi_{\nu+1}$.

With increasing A, the level splitting rapidly increases in a standard way. The behavior of the susceptibilities is more complicated. They cross, but sufficiently close to resonance they repel each other, forming narrow dips (antiresonance) or peaks (resonance). The widths and amplitudes of the dips and peaks display a sharp dependence on the amplitude and frequency of the field.

For weak field, it is straightforward to find the splitting of the susceptibilities,

$$\Delta\chi_{\nu;N}(\omega_F) = |\chi_\nu(\omega_F) - \chi_{\nu+\mathrm{sgn}\,N}(\omega_F)|,$$

close to N-photon resonance between states $|m\rangle^{(0)}$ and $|m+N\rangle^{(0)}$. In this region, the frequency detuning from the resonance,

$$\Delta\omega(m;N) = N(\delta\omega - \delta\omega_{m;N}), \tag{9}$$

is small, $|\Delta\omega(m;N)| \lesssim \Omega_R(m;N)$. To the lowest order in A but for an arbitrary ratio $\Omega_R(m;N)/|\Delta\omega(m;N)|$ the quasienergy states $|\nu\rangle$ and $|\nu+\mathrm{sgn}\,N\rangle$ are linear combinations of the states $|m\rangle^{(0)}$ and $|m+N\rangle^{(0)}$. Then, from Eq. (2) it follows that the splitting of the quasienergies $\Delta\varepsilon_{\nu;N}=|\varepsilon_\nu - \varepsilon_{\nu+\mathrm{sgn}\,N}|$ is

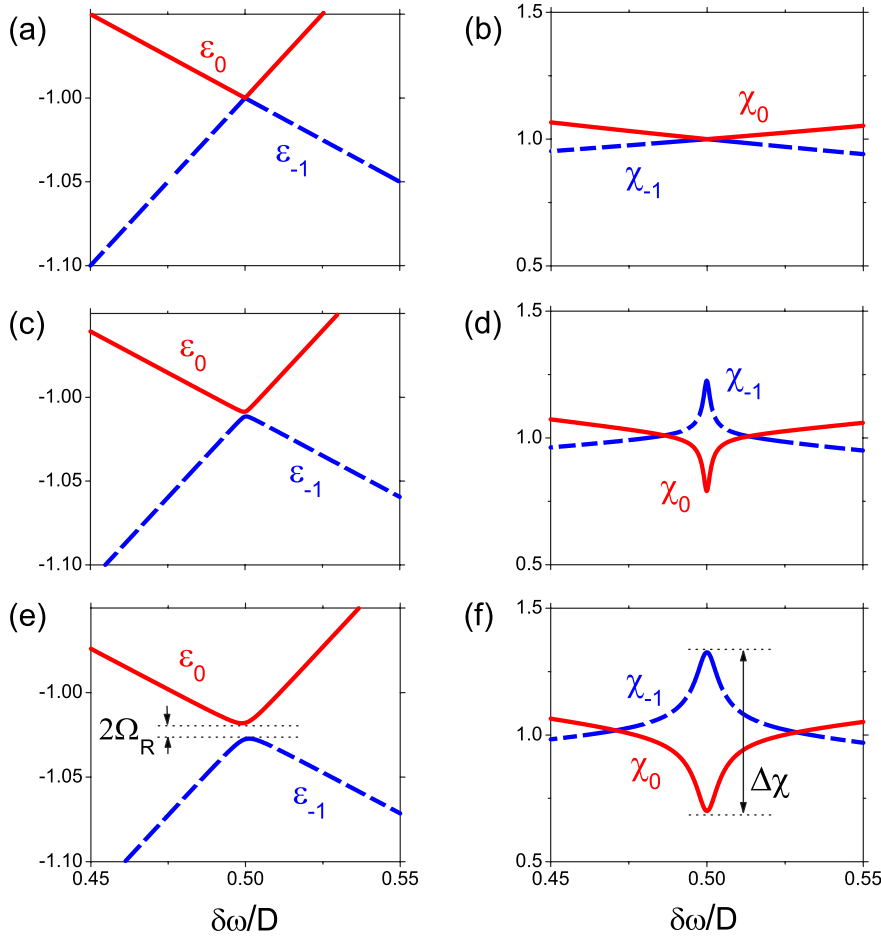$$\Delta\varepsilon_{\nu;N} = [\Delta\omega^2(m;N) + 4\Omega_R^2(m;N)]^{1/2}. \tag{10}$$

FIG. 3. (Color online) Level anticrossing and antiresonance of the susceptibilities. The figure refers to a three-photon resonance, $N=3$, in an $S=2$ system. The involved quasienergy states are $\nu=-1$ and $\nu=0$. The resonating Zeeman states for $A=0$ are $m=-2$ and $m=1$ (the ground and the third excited state). Left and right panels show the quasienergies ε_ν and susceptibilities χ_ν for the same reduced field A/D. Panels (a) and (b), (c) and (d), and (e) and (f) refer to $A/D=0$, 0.2, and 0.3, respectively.

From this expression and Eqs. (4) and (8), it follows that the susceptibility splitting is

$$\Delta\chi_{\nu;N} = \frac{8|N|\Omega_R^2(m;N)}{A^2[\Delta\omega^2(m;N) + 4\Omega_R^2(m;N)]^{1/2}}. \quad (11)$$

The splitting $\Delta\chi_{\nu;N}$ as a function of frequency $\delta\omega$ is maximal at N-photon resonance, $\delta\omega=\delta\omega_{m;N}$. The half-width of the peak of $\Delta\chi_{\nu;N}$ at half height is determined by the Rabi splitting and is equal to $\sqrt{3}\Omega_R/N$. The peak is strongly non-Lorentzian; it is sharper than the Lorentzian curve with the same half-width. This sharpness is indeed seen in Fig. 3. Our numerical results show that Eq. (11) well describes the splitting in the whole frequency range $|\Delta\omega| \lesssim \Omega_R$.

For small A, the susceptibility splitting is stronger than the level repulsion. It follows from Eqs. (10) and (11) that at exact N-photon resonance $\Delta\varepsilon \propto A^{|N|}$, whereas $\Delta\chi \propto A^{|N|-2}$. This scaling is seen in Fig. 4. For $A/D \gg 1$, on the other hand, the eigenstates $|\nu\rangle$ become close to the eigenstates of a spin with Hamiltonian $-AS_x/2$. As a result, the susceptibility splitting decreases with increasing A, $|\Delta\chi_{\nu;N}| \propto A^{-1}$; the proportionality coefficient here is independent of N. Therefore, for $N \geq 3$, $\Delta\chi_\nu$ displays a maximum as a function of A, as seen in Fig. 4.

Two-photon resonance

As mentioned above, the lowest-order perturbation theory [Eq. (7)] does not describe resonant susceptibility for two-photon resonance. Indeed, it follows from Eq. (11) that at exact resonance, $\delta\omega=\delta\omega(m;2)$, the susceptibility splitting for weak fields is

$$\Delta\chi_{\nu;2} = D^{-1}[(S-m-1)(S-m)(S+m+1)(S+m+2)]^{1/2}. \quad (12)$$

This splitting is independent of A. The expression for the susceptibility (7) is also independent of A, yet it does not
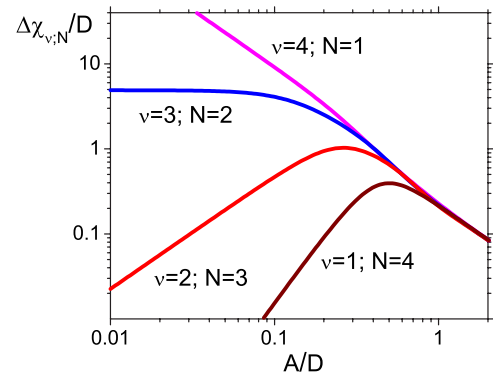

FIG. 4. (Color online) The multiphoton susceptibility splitting for $S=2$. The curves refer to exact N-photon resonances, with $N=1,\ldots,4$, for transitions from the ground Zeeman state $m=-2$ to the excited states $m=-1,\ldots,2$, respectively.

lead to susceptibility splitting and therefore is incorrect at two-photon resonance.

The inapplicability of the simple perturbation theory [Eq. (7)] is a consequence of quantum interference of transitions, the effect known in the linear response of multilevel systems.[16] To the leading order in A, the susceptibility is determined by the squared amplitudes of virtual transitions to neighboring states. For a two-photon resonance, $\delta\omega = \delta\omega_{m;2}$, the distances between the levels involved in the transitions $|m\rangle^{(0)} \to |m+1\rangle^{(0)}$ and $|m+2\rangle^{(0)} \to |m+1\rangle^{(0)}$ are equal, $\varepsilon^{(0)}(m+1) - \varepsilon^{(0)}(m) = \varepsilon^{(0)}(m+1) - \varepsilon^{(0)}(m+2)$. Therefore, the transitions resonate and interfere with each other.

To calculate the susceptibility, it is necessary to start with a superposition of states $|m\rangle^{(0)}$ and $|m+2\rangle^{(0)}$, add the appropriately weighted amplitudes of transitions $|m\rangle^{(0)} \to |m+1\rangle^{(0)}$ and $|m+2\rangle^{(0)} \to |m+1\rangle^{(0)}$, and then square the result. This gives the correct answer. The independence of the susceptibility splitting from A for two-photon resonance in the range of small A as given by Eq. (12) is seen in Fig. 4.

IV. SUSCEPTIBILITY CROSSING FOR A SEMICLASSICAL SPIN

The analysis of the simultaneous level and susceptibility crossing is particularly interesting and revealing for large spins and for multiphoton transitions with large N. For $S \gg 1$, the spin dynamics can be described in the WKB approximation. We will start with the classical limit. In this limit, it is convenient to use a unit vector $\mathbf{s} = \mathbf{S}/S$, with $\mathbf{s} \equiv (s_x, s_y, s_z) \equiv (\sin\theta\cos\phi, \sin\theta\sin\phi, \cos\theta)$, where θ and ϕ are the polar and azimuthal angles of the vector $\mathbf{s}$. To the lowest order in S^{-1}, equations of motion for the spin components can be written as

$$\dot{s}_x = s_y(s_z + \mu), \quad \dot{s}_y = -s_x(s_z + \mu) + fs_z,$$

$$\dot{s}_z = -fs_y, \quad f = A/2SD, \quad \mu = \delta\omega/SD. \quad (13)$$

Here, overdot implies differentiation with respect to dimensionless time $\tau = SDt$, that is, $\dot{\mathbf{s}} \equiv d\mathbf{s}/d\tau = (SD)^{-1}d\mathbf{s}/dt$. Equations (13) preserve the length of the vector $\mathbf{s}$ and also the reduced Hamiltonian $g = H/S^2D$,

$$g \equiv g(\theta,\phi) = -\frac{1}{2}(s_z + \mu)^2 - fs_x. \quad (14)$$

For convenience, we added to g the term $-\mu^2/2$.

The effective energy $g(\theta,\phi)$ is shown in Fig. 5. Also shown in this figure are the positions of the stationary states $\dot{\mathbf{s}} = \mathbf{0}$ and examples of the phase trajectories described by Eqs. (13).

An insight into the spin dynamics can be gained by noticing that g has the form of the scaled free energy of an easy-axis ferromagnet,[17] with $\mathbf{s}$ playing the role of the magnetization $\mathbf{M}/M$ and with μ and f being the reduced components of the magnetic field along the easy axis z and the transverse axis x, respectively. In the region
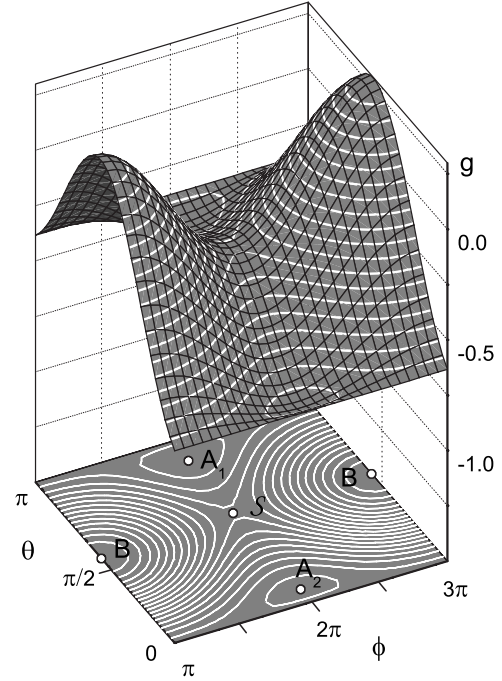

FIG. 5. The effective energy $g(\theta,\phi)$ as a function of the polar and azimuthal angles of the classical spin θ and ϕ. The lines $g(\theta,\phi) = \text{const}$ describe classical spin trajectories. The points A_1 and A_2 are the minima of g, B is the maximum, and $\mathcal{S}$ is the saddle point. In the region $g_{\mathcal{S}} > g > g_{A_1}$, there are two coexisting types of trajectories. They lie on the opposite sides of the surface $g(\theta,\phi)$ with respect to $g_{\mathcal{S}}$. The plot refers to $\mu = 0.125$, $f = 0.3$.

$$|f|^{2/3} + |\mu|^{2/3} < 1, \quad (15)$$

the function g has two minima, A_1 and A_2, a maximum B, and a saddle point $\mathcal{S}$. We will assume that the minimum A_2 is deeper than A_1, that is,

$$g_B > g_{\mathcal{S}} > g_{A_1} > g_{A_2}. \quad (16)$$

As seen from Eqs. (13) and (14) and Fig. 5, for $f > 0$ the minima and the saddle point are located at $\phi = 0$ and the maximum is at $\phi = \pi$; the case $f < 0$ corresponds to a replacement $\phi \to \phi + \pi$. On the boundary of the hysteresis region [Eq. (15)], the shallower minimum A_1 merges with the saddle point $\mathcal{S}$.

In the case of an easy-axis ferromagnet with free energy g, the minima of g correspond to coexisting states of magnetization within the hysteresis region [Eq. (15)]. For multiphoton absorption, g is the scaled quasienergy, not the free energy, and stability is determined dynamically by balance between relaxation and high-frequency excitation. One can show that for relevant energy relaxation mechanisms, the system still has coexisting stable stationary states albeit only in a part of the hysteresis region [Eq. (15)]. The states correspond to one or both minima and the maximum of g; for small damping, the actual stable states are slightly shifted away from the extrema of g on the (θ,ϕ) plane. We will not discuss relaxation effects in this paper.

A. Conformal property of classical trajectories

Dynamical trajectories of a classical spin on the plane (θ, ϕ) are the lines $g(\theta, \phi) = \text{const}$. They are either closed orbits around one of the minima A_1 and A_2 or the maximum B of g, or open orbits along the ϕ axis (see Fig. 5). On the Bloch sphere $\mathbf{s}^2 = 1$, closed orbits correspond to precession of the unit vector $\mathbf{s}$ around the points $\mathbf{s}_{A_1}$, $\mathbf{s}_{A_2}$, or $\mathbf{s}_B$, in which $\mathbf{s}$ does not make a complete turn around the polar axis. Open orbits correspond to spinning of $\mathbf{s}$ around the polar axis accompanied by oscillations of the polar angle θ. Even though the spin has three components, the spin dynamics is the dynamics with one degree of freedom and the orbits on the Bloch sphere do not cross.

An important feature of the dynamics of a classical spin in the hysteresis region is that, for each g in the interval (g_{A_1}, g_S), the spin has two coexisting orbits (see Fig. 5). One of them corresponds to spin precession around $\mathbf{s}_{A_1}$. It can be a closed loop or an open trajectory around the point A_1 on the (θ, ϕ) plane. The other is an open trajectory on the opposite side of the g surface with respect to the saddle point. We will classify them as orbits of types I and II, respectively.

We show in the Appendix that classical equations of motion can be solved in an explicit form and the time dependence $\mathbf{s}(\tau)$ is described by the Jacobi elliptic functions. The solution has special symmetry. It is related to the conformal property of the mapping of s_z onto τ. The major results of the analysis are the following features of the trajectories $\mathbf{s}(\tau)$ of types I and II: for equal g, (i) their dimensionless oscillation frequencies $\omega(g)$ are equal to each other, and (ii) the period-averaged values of the component $s_x(\tau)$ are equal, too,

$$\omega_I(g) = \omega_{II}(g), \quad \langle s_x(\tau) \rangle_I = \langle s_x(\tau) \rangle_{II}. \tag{17}$$

Here, the subscripts I and II indicate the trajectory type. The angular brackets $\langle \cdots \rangle$ imply period averaging on a trajectory with a given g.

The quantity $\langle s_x(\tau) \rangle$ gives the classical response of the spin to the field $\propto A$. Equation (17) shows that this response is equal for the trajectories with equal values of the effective Hamiltonian function g. This result holds for any field amplitude A; it is by no means limited to small A/D where the perturbation theory in A applies.

B. WKB picture in the neglect of tunneling

In the WKB approximation, the values of quasienergy ε_ν in the neglect of tunneling can be found by quantizing classical orbits $g(\theta, \phi) = \text{const}$ (see Ref. 18 and papers cited therein). Such quantization should be done both for orbits of type I and type II, and we classify the resulting states as the states of type I and type II, respectively. The distance between the states of the same type in energy units is $\hbar \omega(g) S D$.[19] Transitions between states of types I and II with the same g are due to tunneling.

If we disregard tunneling, the quasienergy levels of states I and II will cross, for certain values of μ. Remarkably, if two levels cross for a given μ, then all levels in the range $g_{A_1} < g < g_S$ cross pairwise. This is due to the fact that the frequencies $\omega(g)$ and thus the interlevel distances for the two

sets of states are the same [see Eq. (17)]. Such simultaneous degeneracy of multiple pairs of levels agrees with the result of the low-order quantum perturbation theory in A and with numerical calculations.

In the WKB approximation, the expectation value of an operator in a quantum state is equal to the period-averaged value of the corresponding classical quantity along the appropriate classical orbit.[19] Therefore, if semiclassical states of types I and II have the same g, the expectation values of the operator S_x in these states are the same according to Eq. (17). Thus, the WKB theory predicts that, in the neglect of tunneling, there occurs simultaneous crossing of quasienergy levels and susceptibilities for all pairs of states with quasienergies between g_{A_1} and g_S. This is in agreement with the result of the perturbation theory in A and with numerical calculations. However, we emphasize that the WKB theory is not limited to small A, and the WKB analysis reveals the symmetry leading to the simultaneous crossing of quasienergy levels and the susceptibilities.

Tunneling between semiclassical states with equal g leads to level repulsion and susceptibility antiresonance. The level splitting $2\Omega_R$ can be calculated by appropriately generalizing the standard WKB technique, for example, as it was done in the analysis of tunneling between quasienergy states of a modulated oscillator.[4] Then, the resonant susceptibility splitting can be found from Eq. (8). The corresponding calculation is beyond the scope of this paper.

V. DEGENERACY LIFTING BY HIGHER-ORDER TERMS IN S_z

The simultaneous crossing of quasienergy levels and susceptibilities in the neglect of tunneling is a feature of the spin dynamics described by Hamiltonian (2). Higher-order terms in S_z lift both this degeneracy and the property that many quasienergy levels are pairwise degenerate for the same values of the frequency detuning $\delta\omega$. The effect is seen already if we incorporate the term S_z^4 in the anisotropy energy, i.e., for a spin with Hamiltonian

$$\tilde{H} = H - \frac{1}{4} G S_z^4. \tag{18}$$

The Hamiltonian $\tilde{H}$ is written in the rotating wave approximation, H is given by Eq. (2), and G is the parameter of quartic anisotropy. The terms S_x^2 and S_y^2 in the spin anisotropy energy do not show up in $\tilde{H}$ even if they are present in the spin Hamiltonian H_0 but the corresponding anisotropy parameters are small compared to ω_0. In the rotating frame, these terms renormalize the coefficient at S_z^2 and lead to fast-oscillating terms $\propto S_\pm^2 \exp(\pm 2i\omega_F t)$ that we disregard.

Multiple pairwise degeneracy occurs where the condition on Zeeman quasienergies $\varepsilon^{(0)}(m) = \varepsilon^{(0)}(m')$ is simultaneously met for several pairs (m, m'). For $G \neq 0$, this happens for $\delta\omega = 0$, that is, when the modulation frequency ω_F is equal to the Larmor frequency ω_0. In this case, the resonating Zeeman states are $|m\rangle^{(0)}$ and $|-m\rangle^{(0)}$ with the same m. The susceptibilities of these states are equal by symmetry with respect to reflection in the plane (x, y).
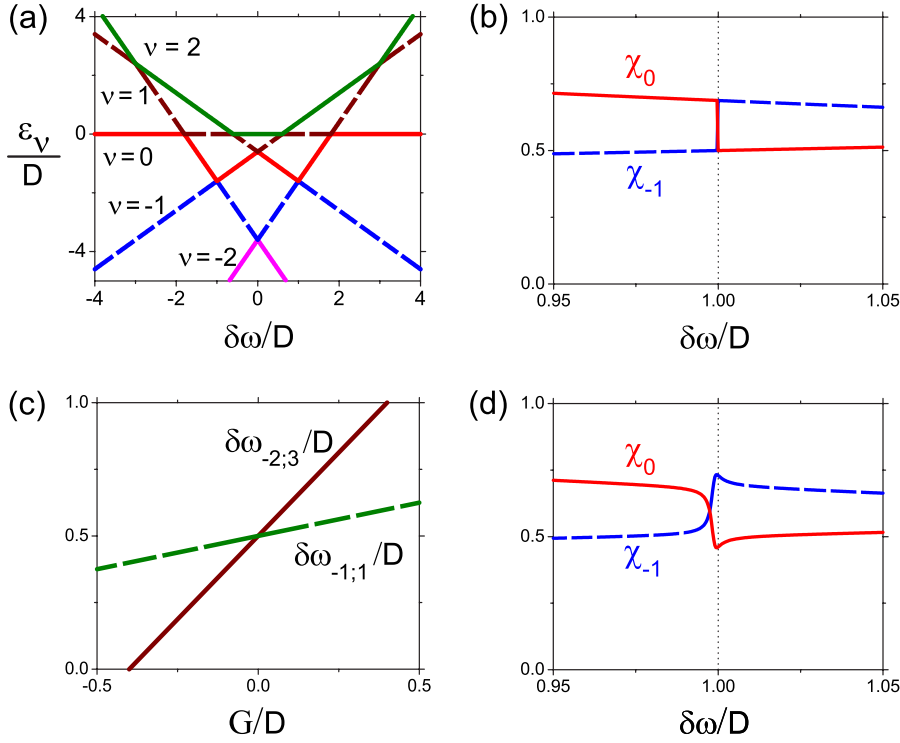
FIG. 6. (Color online) Quasienergy and susceptibility switching for a spin $S=2$ with quartic in S_z anisotropy. Panels (a), (b), and (d) refer to the dimensionless quartic anisotropy parameter $G/D=0.4$ in Eq. (18). Panels (b) and (d) refer to the three-photon resonance $|-2\rangle^{(0)} \rightarrow |1\rangle^{(0)}$ with the scaled modulation amplitude $A/D \rightarrow 0$ and $A/D=0.3$, respectively; the dotted line shows the position of the resonance $\delta\omega/D=1$. Panel (c) shows the dependence of the resonant frequency detuning $\delta\omega_{m;N}$ on the higher-order anisotropy parameter G in the limit $A \rightarrow 0$.

N-photon resonance for nonzero G and $\omega_F \neq \omega_0$ occurs generally only for one pair of states $|m\rangle^{(0)}$ and $|m+N\rangle^{(0)}$. This is seen in panel (a) in Fig. 6. With increasing $|G|$, the difference in the resonant values of frequency increases, as seen in panel (c) in the same figure.

The susceptibilities in resonating states are different in the weak-field limit. When the frequency ω_F adiabatically goes through resonance, there occurs an interchange of states for weak field A: if the state $|\nu\rangle$ was close to $|m\rangle^{(0)}$ on one side of resonance, it becomes close to $|m+N\rangle^{(0)}$ on the other side. As a consequence, the susceptibility χ_ν sharply switches from its value in the state $|m\rangle^{(0)}$ to its value in the state $|m+N\rangle^{(0)}$.

Susceptibility switching is seen in panels (b) and (d) in Fig. 6. For a weak field, the frequency range where the switching occurs is narrow and the switching is sharp (vertical, in the limit $A \rightarrow 0$). As the modulation amplitude A increases, the range of frequency detuning $\delta\omega$ over which the switching occurs broadens. In addition, for small G, the susceptibility displays spikes. They have the same nature as for $G=0$. However, they are much less pronounced, as seen from the comparison of panel (d) in Fig. 6 and panel (f) in Fig. 3 which refer to the same value of A/D.

VI. CONCLUSIONS

In this paper, we have considered a large spin with an easy-axis anisotropy. The spin is in a strong magnetic field along the easy axis and is additionally modulated by a transverse field with frequency ω_F close to the Larmor frequency ω_0. We have studied the coherent resonant response of the spin. It is determined by the expectation value of the spin component transverse to the easy axis. We are interested in multiphoton resonance where $N\omega_F$ coincides or is very close to the difference of the Zeeman energies $E_{m+N}^{(0)} - E_m^{(0)}$ in the absence of modulation.

The major results refer to the case where the anisotropy energy is of the form $-DS_z^2/2$. In this case, not only the quasienergies of the resonating Zeeman states $|m\rangle^{(0)}$ and $|m+N\rangle^{(0)}$ cross at multiphoton resonance, but the susceptibilities in these states also cross, in the weak-modulation limit. Such crossing occurs simultaneously for several pairs of Zeeman states. As the modulation amplitude A increases, the levels are Stark shifted and the susceptibilities are also changed. However, as long as the Rabi splitting due to resonant multiphoton transitions (tunneling) can be disregarded, for resonant frequency the quasienergy levels remain pairwise degenerate and the susceptibilities remain crossing. We show that this effect is nonperturbative in A and that it is due to the special conformal property of the classical spin dynamics.

Resonant multiphoton transitions lift the degeneracy of quasienergy levels, leading to a standard level anticrossing. In contrast, the susceptibilities as functions of frequency cross each other. However, near resonance they display spikes. The spikes of the corresponding susceptibilities point in the opposite direction, leading to a decrease (antiresonance) or an increase (resonance) of the response. They have a profoundly non-Lorentzian shape [Eq. (11)], with width and height that strongly depend on A. The spikes can be observed by adiabatically sweeping the modulation frequency through a multiphoton resonance. If the spin is initially in the ground state, a sequence of such sweeps allows one to study the susceptibility in any excited state provided the relaxation time is long enough.

The behavior of the susceptibilities changes if terms of higher order in S_z in the anisotropy energy are substantial. In this case, crossing of quasienergy levels is not accompanied

by crossing of the susceptibilities in the limit $A \to 0$. Resonant multiphoton transitions lead to steplike switching between the branches of the susceptibilities of the resonating Zeeman states. Still, the susceptibilities display spikes as functions of frequency for a sufficiently strong modulating field.

The results of the paper can also be applied to molecular magnets in a static magnetic field. The spin Hamiltonian in the rotating wave approximation [Eq. (2)] is similar to the Hamiltonian of a spin in a comparatively weak static field, with the Larmor frequency $\delta\omega$ of the same order as the anisotropy parameter D. The susceptibility then characterizes the response to the field component transverse to the easy axis. Quasienergies $\varepsilon^{(0)}(m)$ are now spin energies in the absence of the transverse field, and instead of multiphoton resonance we have resonant tunneling. Our results show that a transverse field does not change the value of the longitudinal field for which the energy levels cross, in the neglect of tunneling. This explains the experiment[10] where such behavior was observed.

In conclusion, we have studied multiphoton resonance in large-spin systems. We have shown that the coherent nonlinear response of the spin displays spikes when the modulation frequency goes through resonance. The spikes have non-Lorentzian shape which strongly depends on the modulation amplitude. The results bear on the dynamics of molecular magnets in a static magnetic field and provide an explanation of the experiment.

ACKNOWLEDGMENTS

APPENDIX: SYMMETRY OF CLASSICAL SPIN DYNAMICS: A FEATURE OF THE CONFORMAL MAPPING

Classical equations of motion for the spin components (13) can be solved in the explicit form, taking into account that $\mathbf{s}^2 = 1$ and that $g(\theta, \phi) = \text{const}$ on a classical trajectory. For time evolution of the z component of the spin, we obtain

$$s_z(\tau) = \frac{r_2(r_1 - r_3) - r_3(r_1 - r_2)\text{sn}^2(u; m_J)}{r_1 - r_3 - (r_1 - r_2)\text{sn}^2(u; m_J)}, \quad (A1)$$

where $r_1 > r_2 > r_3 > r_4$ are the roots of the equation

$$[(r + \mu)^2 + 2g]^2 + 4f^2(r^2 - 1) = 0 \quad (A2)$$

and $\text{sn}(u; m_J)$ is the Jacobi elliptic function. The argument u and the parameter m_J are

$$u = \tilde\omega\tau, \quad \tilde\omega = \frac{1}{4}[(r_1 - r_3)(r_2 - r_4)]^{1/2},$$

$$m_J = (r_1 - r_2)(r_3 - r_4)/(r_1 - r_3)(r_2 - r_4). \quad (A3)$$

Equation (A1) describes an orbit which, for a given g, oscillates between $s_z = r_1$ and $s_z = r_2$; the corresponding oscillations
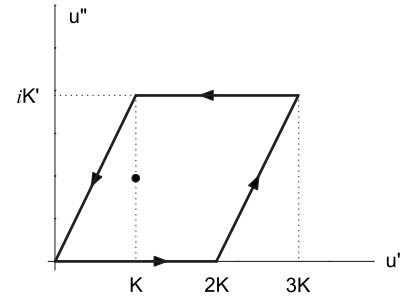

FIG. 7. The contour of integration in the $u \propto \tau$ plane. The horizontal parts correspond to two trajectories $\mathbf{s}(\tau)$ with the same g. The values of $\mathbf{s}(\tau)$ on the tilted parts of the parallelogram are the same. The plot refers to $\mu = 0.125$, $f = 0.3$, $g = -0.366$.

of s_x, s_y can be easily found from Eqs. (13) and (14).

Oscillations of s_z between r_3 and r_4 for the same g are also described by Eq. (A1) provided one replaces $u \to u + K(m_J) + iK'(m_J)$, where $K(m_J)$ is the elliptic integral and $K'(m_J) = K(1 - m_J)$. Clearly, both types of oscillations have the same period over τ equal to $2K(m_J)/\tilde\omega$. They correspond, respectively, to the trajectories of types II and I in Fig. 5 that lie on different sides of the $g(\theta, \phi)$ surface. As a consequence, the vibration frequencies for the trajectories $\omega_I(g)$ and $\omega_{II}(g)$ are the same. This proves the first relation in Eq. (17).

The Jacobi elliptic functions are double periodic, and therefore s_z is also double periodic,

$$s_z(\tau) = s_z[\tau + \tilde\omega^{-1}(2nK + 2imK')], \quad (A4)$$

with integer n, m. Ultimately, this is related to the fact that equations of motion (13) after simple transformations can be put into a form of a Schwartz-Christoffel integral that performs conformal mapping of the half-plane $\text{Im } s_z > 0$ onto a rectangle on the u plane. We will show now that the mapping has a special property that leads to equal period-averaged values of $s_x(\tau)$ on trajectories of different types but with the same g. Because $s_z(\tau)$ is double periodic [see Eq. (A4)], so is the function $s_x(\tau) = -(2f)^{-1}[2g + (s_z(\tau) + \mu)^2]$. Keeping in mind that the transformation $u \to u + K(m_J) + iK'(m_J)$ moves us from a trajectory with a given g of type I to a trajectory of type II, we can write the difference of the period-averaged values of $s_x(\tau)$ on the two trajectories as

$$\langle s_x(\tau)\rangle_I - \langle s_x(\tau)\rangle_{II} = \frac{\omega(g)}{2\pi\tilde\omega}\oint_C s_x du, \quad (A5)$$

where the contour C is a parallelogram on the u plane with vortices at $0, 2K, 3K + iK', K + iK'$. It is shown in Fig. 7.

An important property of the mapping (A1) is that $s_z(\tau)$ has one simple pole inside the contour C, as marked in Fig. 7. Consequently, $s_x(\tau)$ has a second-order pole. The explicit expression (A1) allows one to find the corresponding residue. A somewhat cumbersome calculation shows that it is equal to zero. Therefore, the period-averaged values of s_x on the trajectories with the same g coincide, thus proving the second relation in Eq. (17).

[1] G. Yusa, K. Muraki, K. Takashina, K. Hashimoto, and Y. Hirayama, Nature (London) **434**, 1001 (2005).

[2] D. M. Larsen and N. Bloembergen, Opt. Commun. **17**, 254 (1976).

[3] V. N. Sazonov and V. I. Finkelstein, Dokl. Akad. Nauk SSSR **231**, 78 (1976).

[4] A. P. Dmitriev and M. I. Dyakonov, Zh. Eksp. Teor. Fiz. **90**, 1430 (1986).

[5] M. I. Dykman and M. V. Fistul, Phys. Rev. B **71**, 140508(R) (2005).

[6] E. M. Chudnovsky and L. Gunther, Phys. Rev. Lett. **60**, 661 (1988).

[7] D. A. Garanin, J. Phys. A **24**, L61 (1991).

[8] A. Garg, Europhys. Lett. **22**, 205 (1993).

[9] J. R. Friedman, M. P. Sarachik, J. Tejada, and R. Ziolo, Phys. Rev. Lett. **76**, 3830 (1996).

[10] J. R. Friedman, M. P. Sarachik, J. M. Hernandez, X. X. Zhang, J. Tejada, E. Molins, and R. Ziolo, J. Appl. Phys. **81**, 3978 (1997).

[11] D. A. Garanin and E. M. Chudnovsky, Phys. Rev. B **56**, 11102 (1997).

[12] W. Wernsdorfer and R. Sessoli, Science **284**, 133 (1999).

[13] A. Garg, Phys. Rev. Lett. **83**, 4385 (1999).

[14] J. Villain and A. Fort, Eur. Phys. J. B **17**, 69 (2000).

[15] W. Wernsdorfer, M. Murugesu, and G. Christou, Phys. Rev. Lett. **96**, 057208 (2006).

[16] M. I. Dykman and M. A. Krivoglaz, *Soviet Physics Reviews* (Harwood Academic, New York, 1984), Vol. 5, pp. 265–441.

[17] L. D. Landau and E. M. Lifshitz, *Electrodynamics of Continuous Media*, 2nd ed. (Elsevier Butterworth-Heinemann, Oxford, 2004).

[18] A. Garg and M. Stone, Phys. Rev. Lett. **92**, 010401 (2004).

[19] L. D. Landau and E. M. Lifshitz, *Quantum Mechanics: Non-relativistic Theory*, 3rd ed. (Butterworth-Heinemann, Oxford, 1981).